Dalton Transactions

PAPER

View Article Online
View Journal | View Issue

Cite this: *Dalton Trans.*, 2016, **45**, 7460

Direct C–C coupling of two Ni-salphen complexes to yield dinickel-disalphen complexes with symmetric and non-symmetric substitution-patterns†

B. E. C. Bugenhagen[a] and M. H. Prosenc*[b]

Received 24th November 2015,
Accepted 16th March 2016

DOI: 10.1039/c5dt04612b

www.rsc.org/dalton

The synthesis of symmetric and non-symmetric 5,5′-linked disalophen Ni(II) complexes by the Suzuki-Miyaura-reaction is reported. Also, the synthesis and structural characterization of four Ni(II)-precursor complexes are presented. The 5-Br-substituted mononuclear complexes **4** and **5** are coupled to the pinacolborane substituted complexes **6** and **7** yielding the four dinuclear dinickel complexes **8–11** in good yields. The crystal structure of dinuclear complex **8** was obtained revealing a coplanar arrangement between the two salophen fragments. Electronic spectra as well as DFT-calculations on the ground states and excitation energies are reported and they reveal a small coupling between the electronically saturated Ni-salophen complexes.

Introduction

Oligonuclear salen-complexes gained a lot of attention recently, owing to their unique combination of an easy-to-modify non-innocent ligand with a very broad range of central metal-ions, ranging from alkali- over 3d metal- to lanthanide-ions.[1,2] Due to this versatility this class of compounds has been investigated for a variety of applications and properties, including metal–organic frameworks,[3,4] catalysis,[5,6] and redox behavior.[7–9] Furthermore, the unique properties of salen-complexes have led to their established role in the research on molecule-based magnetism.[10–13] In a recent study, 5,5′-dibromo-salophen-cobalt(II)-molecules have been oligomerized on a gold-surface in an Ullmann-type coupling reaction under the formation of 5,5′-C–C-coupled oligomeric complex chains.[14] These molecular chains exhibited a unique magnetic behavior, which is caused by the interaction of the magnetic orbitals of the cobalt atoms with the extended π-system of the ligand along the chain.[15] Based on this result, an on-surface hetero-coupling strategy was developed to combine different salophen-building blocks yielding oligonuclear complexes for potential molecular spintronic devices.[16]

A variety of oligonuclear salen- and salophen-complexes are known in the literature, *e.g.* covalently linked oligosalen-,[13,17] fused salen-[18–21] and macrocyclic complexes.[22] Nevertheless, a direct synthetic approach yielding salen-dimers and -oligomers linked *via* a 5,5′-C–C bond has not been reported. As mentioned before, oligosalen-complexes with this particular bonding-pattern may exhibit a unique combination of properties and applications and thus their systematic investigation is of special interest.

For the directed synthesis of multinuclear linked salen complexes, a simple, standardized and versatile synthetic protocol is necessary. Keeping the maximum flexibility of the target compounds in mind, including unsymmetrical substitution patterns of the salen- and salophen ligands, the ideal approach would be a direct cross-coupling reaction of prefabricated building blocks. One example of a direct coupling reaction of two salen-complexes has been reported in the literature, exploiting the olefin-metathesis reaction,[23] but only symmetric salen-complexes were achieved.

In this paper we present a method for the synthesis of symmetric and unsymmetric 5,5′-bonded dinuclear nickel-salophen-complexes by cross-coupling of mononuclear precursor-complex building blocks. In addition, the structural and electronic properties of the synthesized mono- and dinuclear nickel-complexes are investigated, especially regarding the effects of an unsymmetrical substitution-pattern and a potential electronic communication between the salophen moieties.

[a]*Institute for Inorganic and Applied Chemistry, University of Hamburg, Martin-Luther-King-Platz 6, 20146 Hamburg, Germany*
[b]*Institute for Physical Chemistry, TU Kaiserslautern, Erwin-Schrödinger-Str. 52, 67663 Kaiserslautern, Germany. E-mail: prosenc@chemie.uni-kl.de*
† Electronic supplementary information (ESI) available. CCDC 1053849, 1053735, 1053850, 1053745 and 1053865. For ESI and crystallographic data in CIF or other electronic format see DOI: 10.1039/c5dt04612b

Results and discussion

In order to synthesize C–C coupled Ni(II) disalophen complexes we employed the Suzuki-cross-coupling-reaction (Scheme 1) as a versatile method to covalently link two molecules.[24,25] This method was chosen for its tolerance towards functional groups and its relatively mild reaction conditions, potentially allowing the introduction of reactive metal-centers and substituents. Also, the absence of bivalent highly Lewis-acidic metal ions during synthesis that could exchange with the coordinated nickel(II) ion is an advantage over other C–C cross-coupling reactions.

For the Suzuki-coupling the four precursor-complexes **4–7** were synthesized (Scheme 2). Complexes **4** and **5** bear one Br-substituent each, and in **6** and **7**, pinacolborane groups are attached. The latter substituent was chosen over boronic acid for its higher stability and pH-neutrality, which is important regarding the acid-sensitivity of the imine-group in Schiff-base-ligands. The synthesis of the precursors was carried out following the procedure of Kleij *et al.* except for the choice of solvents.[3]

The mono-imines **1** and **2** (Scheme 2) were generated from *ortho*-diaminobenzene and selected salicylic aldehyde bearing one or two *tert*-butyl substituents.[26] The mono-imine (**1** or **2**) was then added to a methanol solution of nickelacetate-tetrahydrate in the presence of triethylamine.[27] Subsequent addition of a solution of either 5-bromosalicylaldehyde or 5-(pinacolboron)-salicylaldehyde (**3**) in THF yielded the corresponding unsymmetrically substituted nickel-salophen precursor complexes **4–7**. Aldehyde **3** was synthesized in a modified literature-protocol from 5-bromosalicylaldehyde.[28] All four precursor complexes were isolated in an analytically pure form in good to excellent yields of 76–99% (see the Experimental section). The Br-substituted complexes **4** and **5** were coupled to the pinacolborane derivatives **6** and **7** with yields given in Table 1.

The cross-coupling reaction was carried out using the complex tetrakistriphenylphosphine palladium(0) as a catalyst in the presence of potassium carbonate as a base. For the reaction, stock-solutions of the precursor-complexes (40 mmol L^{-1}) and the catalyst (10 mmol L^{-1}) in THF were prepared. Similar amounts of a Br-precursor and a BPin-precursor complex were mixed in Schlenk-flasks and then treated with the catalyst

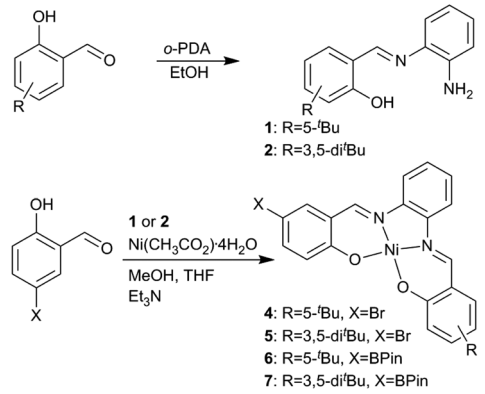

Scheme 2 Two-step synthesis of the nickel-salophen precursors. *o*-PDA = *ortho*-diaminobenzene.

Table 1 Numbers and yields of the coupling-products. The Br-carrying coupling components are in columns, and the pinacolborane in rows

	4	**5**
6	**8**, 56%	**9**, 66%
7	**10**, 66%	**11**, 93%

complex and an aqueous solution of potassium carbonate. After 24 hours of stirring at 70 °C the products were isolated.

Crystallography

Of the four mononuclear complexes **4–7** and the dinuclear complex **8**, single-crystals suitable for structure analysis could be obtained after crystallization from $CHCl_3$/*n*-hexane (**4**), THF/*n*-hexane (**5–7**) or pyridine/*n*-hexane (**8**). The structures of **7** and **8** are presented in Fig. 1. For crystallographic information see Table S1 in the ESI.† Selected bond-lengths are listed in Table S2† along with structural data retrieved from DFT-calculations. In all five complexes the nickel-atom is four coordinate with Ni–N distances from 1.8505(15) Å in **7** to 1.8624(26) Å in **4** and Ni–O distances from 1.8315(13) Å in **7** to 1.8501(22) Å in **4**. These geometry parameters are in accordance with those found in the literature (see Fig. S1†).[29] Remarkably, the Ni–N1 and Ni–O1 bonds are slightly longer

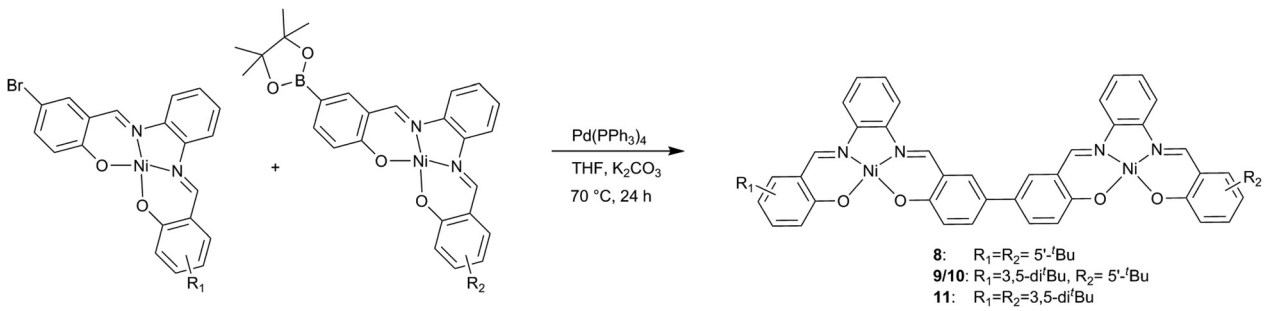

Scheme 1 Suzuki-cross-coupling of two nickel-salophens. R1, R2: 5-^{t}Bu, 3,5-di^{t}Bu.

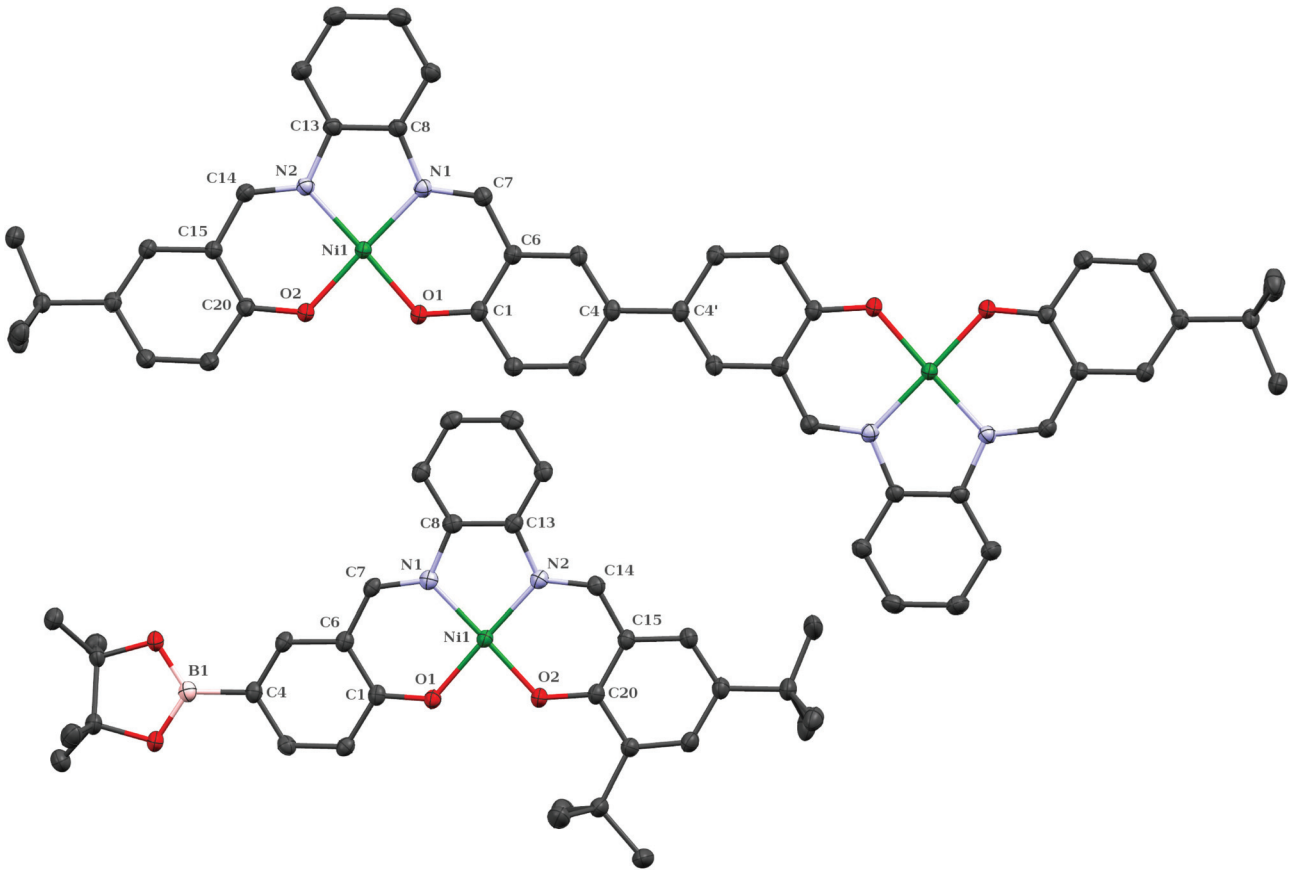

Fig. 1 Top: molecular structure of **8**, bottom: molecular structure of **7**. Hydrogen atoms and solvent-molecules are omitted for clarity; ellipsoids are at 50% probability.

than the corresponding Ni–N2 and Ni–O2 distances with differences ranging from 1.07 pm (**6**) to 0.43 pm (**4**) for the Ni–O distances and from 0.07 pm (**6**) to 0.97 pm (**7**) for the Ni–N bonds. Although this difference is well within the margin of error for compounds **4**, **6** and **8**, the fact that this trend is observed in all five crystal structures as well as reproduced by the DFT calculations makes this observation significant and raises the question of the strength of a substituent influence. The electron-donating character (+I-effect) of the ^{t}Bu-substituents as opposed to the electron-withdrawing substituents (bromine: −I-effect, boron: −M-effect) and the resulting shift of the electron density appear to be the cause.

The structure of the dinuclear complex **8** exhibits a crystallographic center of inversion on the phenyl–phenyl axis and thus the alignment of the phenyl rings is coplanar in the solid state. This conformation is presumably enforced by crystal-packing effects, since the ordering in the crystal is dominated by shifted stacks of salophen-complexes. In these stacks, the C–C-bond of each dimer is sandwiched between two planar salophen units with a distance of 3.57 Å.

The C–C distance between the 6-membered rings in complex **8** is found to be 1.483(3) Å and corresponds to an elongated double-bond between the phenyl ring fragments. This is in accordance with reported structures of biphenyls in the solid state,[30] where the repulsion between the two 6-membered rings leads to a long C–C bond.[31] The salophen-units in **8** take an *anti*-conformation in the solid state.

Spectroscopic characterization and DFT-studies

All four precursor-complexes and the coupling-products **9**/**10** and **11** were subjected to NMR-analysis. Due to the poor solubility of the dinuclear compounds, ^{13}C and correlation spectra (COSY, HMBC, HSQC) were recorded only for the mononuclear compounds with the consequence that an unambiguous assignment of most of the signals was impossible for compounds **9**/**10** and **11**. It catches the eye that the chemical shifts of the imine-protons at the ^{t}Bu-side of the molecule are at lower field than the shifts of the protons at the Br/BPin-side. This permits the assignment of the imine-protons in the spectra of **9**/**10** and **11**. The shift of the imine-protons is also a good indication of the asymmetric substitution-pattern in compound **9**/**10**, since they are split into four clearly distinguishable singlets in the ^{1}H-NMR spectra. For information on peak-assignment, please refer to the ESI (Table S4, Scheme S1†).

The UV/Vis spectra of complexes **4–10** were recorded in THF at room temperature and are depicted in Fig. 2. The data extracted from the spectra are listed in Table 2 and are in

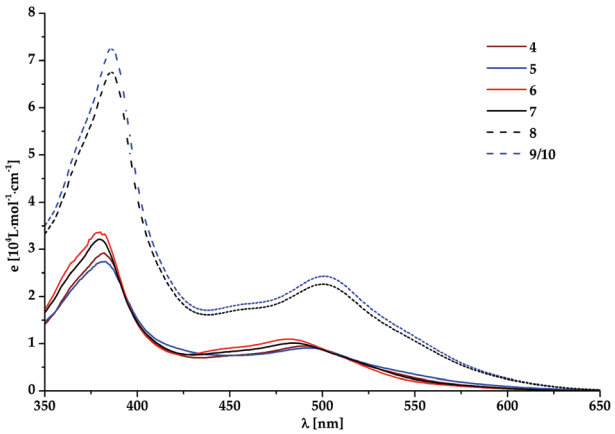

Fig. 2 UV/Vis spectra of compounds **4–9** recorded in THF at room temperature.

Table 2 Absorption maxima and extinction coefficients extracted by Gaussian deconvolution from the electronic spectra of compounds **4–9/10**. λ_{max} are given in nm, and $\varepsilon(\lambda_{max})$ are listed in brackets and are given in 10^4 L mol^{-1} cm^{-1}

	Band #1	Band #2	Band #3	Band #4	Band #5
	$\lambda_{max}(\varepsilon)$	$\lambda_{max}(\varepsilon)$	$\lambda_{max}(\varepsilon)$	$\lambda_{max}(\varepsilon)$	$\lambda_{max}(\varepsilon)$
4	519(3.7)	494(3.5)	445(6.6)	384(6.7)	373(23)
5	530(3.6)	496(3.8)	445(6.8)	383(7.0)	371(20)
6	525(2.6)	491(4.8)	447(7.9)	382(8.2)	370(27)
7	529(2.4)	493(4.8)	445(7.1)	382(8.1)	371(25)
8	534(12)	502(12)	456(16)	387(21)	377(54)
9/10	533(11)	503(8.4)	459(15)	387(19)	376(50)

accordance with spectra from comparable literature-known complexes.[8,32] Peak-positions and absorption-coefficients were obtained by Gaussian deconvolution ($R^2 \geq 99.9\%$) of the recorded spectra (see Fig. S2†). The spectra (Fig. 2) of all the complexes consist of five major absorption bands.

Comparing the spectra of the mononuclear compounds **4–7**, the lowest energy absorption (band #1), a broad band with a maximum between 519 and 530 nm is the only transition that significantly changes throughout the four spectra. The wavelength of this absorption increases in the order **4** < **6** < **7** < **5** in increasing order. This increase indicates that the number of ^{t}Bu-substituents (complexes **5** and **7**) has a larger influence on this absorption band than the nature of the opposite substituent (Br (**4**) or BPin (**6**)). In the spectra of the dinuclear compounds, this band experiences a significant bathochromic shift and is found at 533 and 534 nm. In the dinuclear complexes **8** and **9/10** the absorption bands #2–#5 are shifted bathochromically by about 5 nm in comparison with the mononuclear complexes. This is less than that expected from shifts of conjugated polyphenyls, where the addition of one phenyl-ring results in a bathochromic shift of about 30 nm.[33–35] Additionally, a striking feature of the UV/Vis-spectra is the difference in absorption intensities between the mono- and dinuclear complexes, which roughly double for all the bands, so $\varepsilon_{Ni_2} \sim 2\ \varepsilon_{Ni_1}$. These findings indicate the very weak conjugation of the π-systems of the salophen units; the dinuclear complexes rather behave like two independent complex molecules, which is not expected based on the spectra of polyphenyls. This interpretation is further reinforced by the long phenyl–phenyl-bond of 1.4831 nm found in the crystal structure of **8** and a distortion of the co-planarity in the DFT-optimized gas-phase structure found by a torsion of the phenyl–phenyl-torsion-angle of roughly 36°.

To clarify the nature of the electronic transitions, TD-DFT-calculations were performed (see Computational details),[36] which were successfully employed on related complexes.[15,37–39] In accord with the deconvoluted spectra the calculations revealed five absorptions with significant intensity in the recorded spectral region.

NTO-analyses were performed on the relevant electronic excitations[40] (Fig. 3, 4, S5 and S6†). For the discussion of these results, the co-ordinate-system presented in Fig. 3 will be used.[41] The lowest energy transition #1 appears to be an MLCT from a d_{xz} orbital at the Ni-atom to the π-system of the ligand with a polarization in the *x*-direction.

The occupied NTO for transitions #1 and #2 has small coefficients at the 5-^{t}Bu groups with opposite sign to the C_6-ring coefficient, indicating an antibonding interaction between the substituents and the C_6-ring. This raises the energy of the occupied frontier orbitals and reduces the band-gap of these transitions. This is confirmed by the experimental spectra, where the absorption band #1 is red-shifted by 11 nm (**4** and **5**) or 4 nm (**6** and **7**) on adding one *tert*-butyl-group.[32]

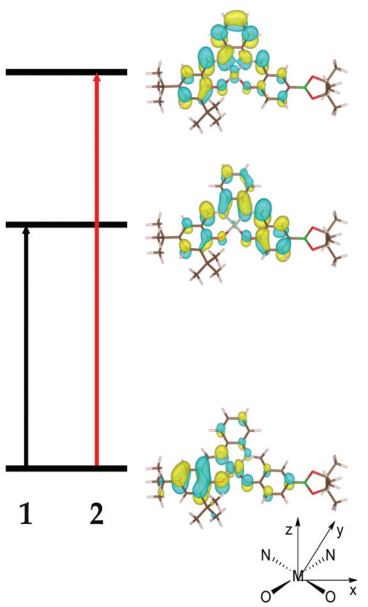

Fig. 3 NTOs for the mononuclear compound **7**. The first two transitions which correspond to bands #1 and #2 in the UV/Vis-spectra are shown. Bottom: the coordinate-system used in the discussion of the electronic transitions. The *z*-axis is perpendicular to the ligand-plane, the *y*-axis lies between the *N*,*N*-ligands, and the *x*-axis lies between the *N*,*O*-ligands.

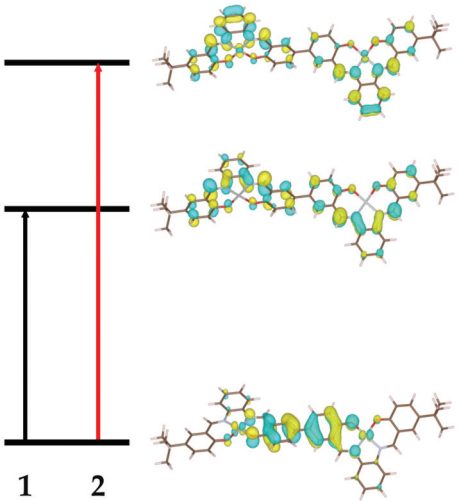

Fig. 4 NTOs for the dinuclear compound **8**. The first two transitions, representing the absorption-bands #1 and #2 observed in the UV/Vis-spectra, are depicted.

The NTO-analysis of the most significant transitions in the dinuclear complex **8** is presented in Fig. 4. For absorptions #1 and #2, transitions from the biphenyl fragment including Ni-d_{xz} orbitals to salophen moieties are observed. This is in accord with transitions calculated for the mononuclear complexes. Due to a small antibonding interaction between the six-membered rings the highest occupied orbital is shifted towards higher energies. This results in smaller HOMO–LUMO-gaps and thus bathochromic shifts of these transitions.

This thesis that the antibonding character of the occupied orbital with respect to the biphenylic bond is responsible for the bathochromic shift of transitions #1 and #2 was further tested. Therefore, we calculated the structure and electronic excitation spectra of the putative complex with all phenyl rings in coplanar arrangement, which should maximize the antibonding interaction between the phenyl rings. The energy calculated for this complex is about +6 kJ mol^{-1} higher than that of complex **8**. A frequency calculation after the geometry optimization revealed one negative force constant for the rotation around the salophen–salophen bond, which indicates the coplanar arrangement to be a transition state for the torsion around the C–C bond.

In the electronic spectrum of the coplanar species obtained by TD-DFT calculations (Fig. S4†), transition #1 appears at an even lower energy than in the TD-DFT-spectrum of the unconstrained compound **8**. The electronic transition #1 in the dinuclear compounds is thus strongly dependent on the rotation-angle of the biphenylic bond. These results would allow tailoring new complexes with respect to optical properties.

Electrochemistry

The redox-behaviour of all four mononuclear compounds (**4**–**7**) and the tetra-*tert*-butyl substituted dinuclear complex (**11**) were investigated. All five substances exhibit two oxidation-steps in the positive potential range (Table 3) in accord with reported complexes.[42,43]

Table 3 Redox waves of compounds **4**–**7** and **11** at a scan rate of 100 mV s^{-1} as referenced to Fc$^+$/Fc

	4	**5**	**6**	**7**	**11**
E_{ox} 1	686	624	681	616	272
E_{red} 1	—[a]	512	—[a]	545	219
$E_{1/2}$ 1	—[b]	568	—[b]	581	250
E_{ox} 2	957	1167[a]	1005	1192	1159

[a] No corresponding reduction signal was detected. [b] Since no corresponding reduction signal was detected, $E_{1/2}$ could not be determined. Potentials are given in mV.

The cyclic voltammograms (Fig. 5) of complexes **5** and **7** show a redox-couple at $E_{1/2}$ = 568 mV and 581 mV respectively. These redox-processes are quasi-reversible according to standard criteria.[44,45] A second irreversible oxidation step is detected at E_{ox} = 1167 mV and E_{ox} = 1192 mV for compounds **5** and **7**. For compounds **4** and **6** two irreversible oxidation steps each were found. The first oxidation steps of **4** and **6** occur at potentials of E_{ox}(4.1) = 686 mV and E_{ox}(6.1) = 681 mV, and the second steps occur at E_{ox}(4.2) = 957 mV and E_{ox}(6.2) = 1005 mV, respectively.

In the cyclic voltammogram of the dinuclear complex **11**, two redox-processes were also observed. The first step at $E_{1/2}$ = 250 mV is found to be quasi-reversible (see also Fig. S15 in the ESI†). The second oxidation occurs at a potential of E_{ox} = 1159 mV and is irreversible. However, due to the very poor solubility of complex **11**, the response was very weak. Since most of the investigated redox-processes are not reversible, we have to limit ourselves to comparing the oxidation-potentials in the following discussion.

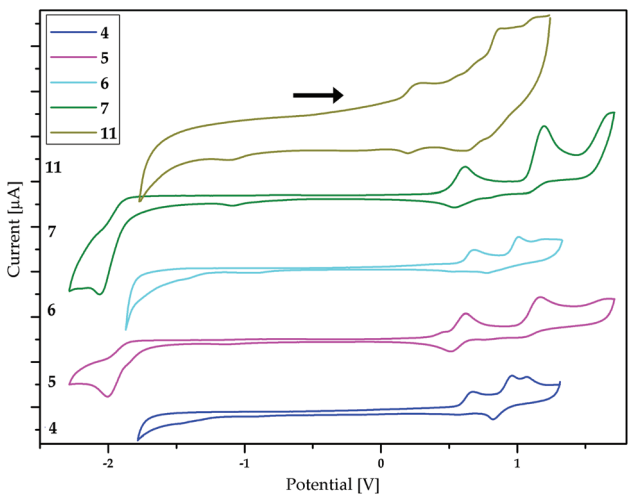

Fig. 5 CV curves of compounds **4**–**7** and **11**. Potentials are measured *vs.* Fc$^+$/Fc. The current of compound **11** was multiplied by a factor of 10 to enhance visibility.

According to the literature, the two abovementioned redox-processes are located at the ligand.[21,42,43] For the mononuclear compounds, the potential of the first oxidation depends mainly on the number of ^{t}Bu-substituents whereas the nature of the other substituent (Br or BPin) has only a minor influence. This is to be expected, since the addition of a substituent with a +I influence like the *tert*-butyl group should shift the oxidation to a more negative potential. This finding is in accord with the results from the electronic spectra. There, a redshift of the first absorption-band for species **5** and **7** is attributed to a higher energy of the highest occupied state due to the second ^{t}Bu-substituent. The first redox-process found for the dinuclear compound **11** occurs at the considerably more negative potential of $E_{ox}(11.1)$ = 272 mV. Keeping in mind that the oxidation is located on the ligand, it may be assumed that for **11** the biphenyl-part of the molecule gets oxidized. This is in accordance with the electronic spectra, where the first electronic transition originates from the highest occupied state with a large coefficient on the biphenyl-bridge. DFT-calculations further reinforce this interpretation: the optimized structure of **11** has a torsion angle of 36° at the biphenyl-bond whereas the structure of the hypothetical cation $\mathbf{11}^+$ is twisted by only 18°, indicating a considerable change in electron density at the biphenyl-unit upon oxidation. Also, the calculated spin-density of the monocation clearly indicates that the first oxidation step takes place at the biphenyl bridge (Fig. S7†).

All the second oxidation-processes in the observed complexes **4–7** and **11** are irreversible. Since compounds **4–7** contain rather reactive substituents (Br and BPin) it can be assumed that at potentials as strong as +1 V, chemical reactions take place.

Conclusions

We presented the first method to synthesize dinuclear salophen-complexes with an unsymmetric substitution pattern by cross-coupling mononuclear salophen building blocks. This method yields a new type of biphenyl-bridged dinuclear salophen complex. The precursor-complexes **4–7** were hitherto unknown, and to the best of our knowledge, compounds **6** and **7** are the first examples of boronate-substituted salophen complexes. Complexes **4–7** were cross-coupled yielding the disalophens **8–11** in good yields.

The complexes were fully characterized including the determination of the crystal structures. Due to the unsymmetrical substitution patterns the mononuclear complexes experience the influence of combined substituent-effects (+M, −M, +I, −I). The substituent effects on the electronic structures of the compounds have been investigated by a combination of X-ray crystallography, cyclic voltammetry and NMR- and UV/Vis-spectroscopy. The experimental results were further evaluated in DFT-calculations. Electronic transitions were further assigned by NTO analyses. From these investigations it can be deduced that the *tert*-butyl substituents have a large influence on optical properties and oxidation potentials due to a shift of the high-lying occupied states towards higher energies. The influence of a Br- as well as a pinacolborane substituent is rather small for the excitation spectra as well as the oxidation potentials. However, the substituents have a large influence on the reversibility of the redox potentials as well as the reactivity of these complexes.

For complex **8** a crystal structure was recorded. It was found that the dinuclear complex **8** is coplanar in the solid state whereas in the DFT-optimized structure-calculations the complex fragments are rotated around the biphenyl axis. The evaluation of the electronic spectra revealed that the dinuclear compounds consist of two electronically weakly coupled salophen units. The filled metal and π-orbitals on the ligand appear to be the cause. From DFT-calculations it can be deduced that upon oxidation of the ligand or excitation from a filled ligand π-orbital with antibonding character with respect to the biphenyl bond the C–C bond is strengthened and the electronic coupling of the two complex fragments increases.

The very successful application of the Suzuki-cross-coupling to the synthesis of sp^2–sp^2-bonded dinuclear salophen complexes opens up the possibility of further exploration of this new class of molecules. Due to the mild conditions of the Suzuki coupling and the simple synthesis of precursor-complexes, this synthetic pathway should allow the fabrication of heterodinuclear complexes or compounds of even higher nuclearity. Research in this direction is currently being carried out by our workgroup.

Experimental section

General considerations

If not mentioned otherwise, all the reactions were performed under normal conditions without the exclusion of oxygen or moisture. The solvents used were of p.a. grade and used as received. Chemicals were purchased from either Sigma-Aldrich or MERCK and used as received.

X-ray crystallography was performed on a Bruker D8 diffractometer with a Bruker Apex 1 camera and an IμS-Mo Kα micro focus source (50 kV, 0.6 mA). Hydrogen-atoms were constrained at fixed positions and refined using the riding-model. A disorder at the pinacolborane-group in the structure of **6** has been treated by using a model consisting of two layers of the carbon-atoms of the pinacolborane-group. Various restraints and constraints were applied.

Infrared spectra were recorded using KBr discs on a Bruker Tensor T7 FT-IR-spectrometer.

The electronic spectra of solutions of compounds **4–10** in THF were recorded on a Varian Cary 50 spectrometer. Extinction coefficients were determined by a serial dilution with five concentrations. Due to low solubility, no meaningful data could be obtained for **11**. For the Gaussian deconvolution of the spectra, the Origin 9.0g software-suite was employed.

NMR spectroscopy was carried out on a Bruker Avance 400 or a Fourier 300 instrument at room temperature with $CDCl_3$ or DMSO-d6 as solvents and referenced to the solvent-signal.

The peaks were assigned according to the numbering-pattern presented in Scheme S1 in the ESI.†

Cyclic voltammetry was performed using a BASi C3 potentiostat. The setup consisted of a 3 mm GC working-electrode, a Pt counter-electrode and an Ag^+/Ag reference-electrode using a Vycore-frit. Where possible, a 1 mM solution in DCM of the compound was measured with 0.1 M TBAP as the supporting electrolyte.

Synthesis of precursors and complexes

Synthesis of 5-(4,4,5,5-tetramethyl-1,3,2-dioxaborolan-2-yl)-salicylaldehyde (3). Under the exclusion oxygen, 4-bromosalicylaldehyde (10.45 g, 35.77 mmol), bis(pinacolato)diboron (13.83 g, 54.46 mmol), sodium acetate (18.50 g, 136.1 mmol) and PEG600 (200 mL) were put into a flask and heated to 70 °C. After degassing the mixture for 20 min, tetrakis-triphenylphosphinepalladium(0) (1.44 g, 1.25 mmol) was added. The reaction mixture was then stirred for 24 h at 70 °C. After extraction with water/ethyl acetate the raw product was purified by column chromatography (PE/EE, silica gel) and recrystallization from hot *n*-heptane. A colourless, crystalline product (4.44 g, 17.9 mmol, yield: 50%) was obtained.

^{1}H NMR (400 MHz, DMSO-d_6, 25 °C): δ 11.09 (bs, 1H, O**H**), 10.27 (s, 1H, **H7**), 8.00 (d, 1H, $^4J_{H3–H5}$ = 1.6 Hz, **H3**), 7.76 (dd, 1H, $^3J_{H6–H5}$ = 8.3 Hz, $^4J_{H3–H5}$ = 1.8 Hz, **H5**), 6.99 (d, 1H, $^3J_{H6–H5}$ = 8.3 Hz, **H6**), 1.28 (s, 12H, **H9**).

General procedure for the preparation of mononuclear salophenato-nickel(II)-complexes

Equimolar amounts of the monoimine (**1** or **2**) and nickel(II) acetate-tetrahydrate were combined in a flask and treated with 2 mL triethylamine. 15 mL of methanol were added afterwards. After five minutes of stirring, a solution of one aliquot of salicylaldehyde in 5 mL of tetrahydrofuran was added. The mixture was stirred overnight, the solvent removed *in vacuo*, and the residue suspended in methanol and then treated with water. The red precipitate was filtered off and washed with methanol and diethyl ether and dried *in vacuo*.

Synthesis of *N*-(5-*tert*-butylsalicylidene)-*N'*-(5-bromosalicylidene)phenylenediaminato nickel(II) (4). This substance was synthesized according to the general procedure for the preparation of salophenato-nickel(II)-complexes (v.s.). Monoimine **1**: 985 mg, 3.67 mmol, nickelacetate-tetrahydrate: 1016 mg, 4.08 mmol, 5-bromosalicylaldehyde: 799 mg, 3.98 mmol. Yield: 1720 mg, 3.39 mmol, 92.2%.

^{1}H NMR (300 MHz, THF-d_8, 25 °C): δ 8.56 (s, 1H, **H7**), 8.50 (s, 1H, **H14**), 7.94–7.92 (m, 2H, **H9 + H12**), 7.54 (d, $^4J_{H3–H5}$ = 2.7 Hz, 1H, **H5**), 7.36 (dd, $^3J_{H18–H19}$ = 8.7 Hz, $^4J_{H16–H18}$ = 2.6 Hz, 1H, **H18**), 7.35 (s, 1H, **H16**), 7.23 (dd, $^3J_{H2–H3}$ = 9.2 Hz, $^4J_{H3–H5}$ = 2.6 Hz, 1H, **H3**), 7.25–7.15 (m, 3H, **H10 + H11**), 6.84 (d, $^3J_{H18–H19}$ = 8.7 Hz, 1H, **H19**), 6.79 (d, $^3J_{H2–H3}$ = 9.2 Hz, 1H, **H2**), 1.30 (s, 9H, **H22**).

^{13}C NMR (75 MHz, THF-d_8, 25 °C): δ 156.1 (**C14**), 155.4 (**C7**), 137.8 (**C17**), 136.7 (**C3**), 133.4 (**C18**), 134.5 (**C5**), 128.2 (**C16**), 127.3 + 126.6 (**C10 + C11**), 124.1 (**C2**), 122.9 (**C6**), 120.6 (**C15**), 121.7 (**C19**), 115.1 + 115.3 (**C9 + C12**), 106.3 (**C4**), 34.7 (1C, **C21**), 31.6 (4C, **C22**).

MS (ESI+, HRMS) *m*/*z* 507.0233 $[M + H]^+$ (calc.: 507.0218).

Elemental analysis: found: C 56.7, H 4.17, N 5.51, O 6.30 (calculated: C 56.7, H 4.20, N 5.63, O 6.30).

Synthesis of *N*-(3,5-di-*tert*-butylsalicylidene)-*N'*-(5-bromosalicylidene)phenylene-diaminato nickel(II) (5). This substance was synthesized according to the general procedure for the preparation of salophenato-nickel(II)-complexes (v.s.). Monoimine **2**: 499 mg, 1.54 mmol, nickelacetate-tetrahydrate: 390 mg, 1.57 mmol, 5-bromosalicylaldehyde: 310 mg, 1.54 mmol. Yield: 721 mg, 1.28 mmol, 83.1%.

^{1}H NMR (300 MHz, THF-d_8, 25 °C): δ 8.60 (s, 1H, **H7**), 8.47 (s, 1H, **H14**), 7.94–7.90 (m, 2H, **H9 + 12**), 7.55 (d, $^4J_{H–H}$ = 2.7 Hz, 1H, **H5**), 7.39 (d, $^4J_{H–H}$ = 2.6 Hz, 1H, **H18**), 7.25 (dd, $J_{H–H}$ = 9.2 Hz, $^4J_{H–H}$ = 2.8 Hz, 1H, **H3**), 7.25–7.16 (m, 3H, **H10 + H11 + H16**), 6.77 (d, $^3J_{H–H}$ = 9.1 Hz, **H2**), 1.45 (s, 9H, **H24**), 1.31 (s, 9H, **H22**).

^{13}C NMR (75 MHz, THF-d_8, 25 °C): δ 166.8 (1C, **C1**), 166.3 (1C, **C20**), 155.9 (1C, **C14**), 154.9 (1C, **C7**), 142–144 (2C, **C8 + C13**), 141.1 (1C, **C19**), 137.4 (1C, **C3**), 137.1 (1C, **C17**), 135.3 (1C, **C5**), 130.6 (1C, **C18**), 128.1 (1C, **C10/C11**), 127.3 (1C, **C16**), 127.2 (1C, **C11/C10**), 124.0 (1C, **C2**), 122.4 (1C, **C6**), 120.6 (1C, **C15**), 116.0 (1C, **C9/C12**), 115.8 (1C, **C12/C9**), 106.0 (1C, **C4**), 36.3 (1C, **C23**), 34.7 (1C, **C21**), 31.4 (4C, **C22**), 29.7 (4C, **C24**).

MS (ESI+, HRMS) *m*/*z* 563.0871 $[M + H]^+$ (calc.: 563.0844).

Elemental analysis: found: C 59.6, H 5.18, N 4.97, O 5.67 (calculated: C 59.7, H 5.20, N 5.01, O 5.67).

Synthesis of *N*-(5-*tert*-butylsalicylidene)-*N'*-(5-(4,4,5,5,-tetramethyl-1,3,2-dioxaborolan-2-yl)salicylidene)phenylenediaminato nickel(II) (6). This substance was synthesized according to the general procedure for the preparation of salophenato-nickel(II)-complexes (v.s.). Monoimine **1**: 411 mg, 1.53 mmol, nickelacetate-tetrahydrate: 390 mg, 1.57 mmol, salicylaldehyde **3**: 378 mg, 1.52 mmol. Yield: 612 mg, 1.16 mmol, 75.9%.

^{1}H NMR (300 MHz, THF-d_8, 25 °C): δ 8.62 (s, 1H, **H7**), 8.56 (s, 1H, **H14**), 8.00–7.94 (m, 2H, **H6 + H12**), 7.92 (d, 1H, $^4J_{H3–H5}$ = 1.6 Hz, **H5**), 7.53 (dd, $^3J_{H3–H2}$ = 8.7 Hz, $^4J_{H3–H5}$ = 1.7 Hz, **H3**), 7.37 (s, 1H, **H16**), 7.35 (dd, 1H, $^3J_{H18–H19}$ = 9.8 Hz, $^4J_{H16–H18}$ = 2.6 Hz, **H18**), 7.24–7.17 (m, 2H, **H10 + H11**), 6.85 (d, 1H, $^3J_{H18–H19}$ = 9.1 Hz, **H19**), 6.84 (d, 1H, $^3J_{H2–H3}$ = 8.7 Hz, **H2**), 1.31 (s, 12H, **H24**), 1.29 (s, 9H, **H22**).

^{13}C NMR (75 MHz, THF-d_8, 25 °C): δ 169.8 (**C1**), 166.4 (**C20**), 156.2 (**C7**), 155.8 (**C14**), 144.3 (**C8** + **C13**), 143.7 (**C5**), 140.6 (**C3**), 137.8 (**C17**), 134.1 (**C18**), 129.1 (**C16**), 127.8 + 127.5 (**C10** + **C11**), 121.5 + 121.1 (**C2** + **C19**), 120.2 (**C15**), 116.1 + 116.0 (**C9** + **C12**), 83.9 (**C23**), 34.5 (**C21**), 34.1 (**C24**), 25.1 (**C22**).

MS (FAB^+, HRMS) *m*/*z* 555.1983 $[M + H]^+$ (calculated: 555.1965).

Elemental analysis: found: C 64.8, H 6.00, N 5.01, O 11.3 (calculated: C 64.9, H 5.99, N 5.05, O 11.5).

Synthesis of *N*-(3,5-di-*tert*-butylsalicylidene)-*N'*-(5-(4,4,5,5,-tetramethyl-1,3,2-dioxa-borolan-2-yl)salicylidene)phenylene-diaminato nickel(II) (7). This substance was synthesized according to the general procedure for the preparation of salophenato-nickel(II)-complexes (v.s.). Monoimine **2**: 513 mg, 1.58 mmol,

nickelacetate-tetrahydrate: 398 mg, 1.60 mmol, salicylaldehyde **3**: 383 mg, 1.31 mmol. Yield: 695 mg, 1.31 mmol, 99.8%.

^{1}H NMR (300 MHz, THF-d$_8$, 25 °C): δ 8.67 (s, 1H, **H7**), 8.52 (s, 1H, **H14**), 7.95 (d, 1H, $^4J_{H3–H5}$ = 2.0 Hz, **H5**), 8.00–7.94 (m, 3H, **H9 + H12**), 7.55 (dd, 1H, $^3J_{H2–H3}$ = 8.7 Hz, $^4J_{H3–H5}$ = 1.8 Hz, **C3**), 7.39 (d, 1H, $^4J_{H16–H18}$ = 2.6 Hz, **H18**), 7.23 (d, 1H, $^4J_{H16–H18}$ = 2.6 Hz, **H16**), 7.26–7.20 (m, 2H, **H10 + H11**), 6.84 (d, 1H, $^3J_{H2–H3}$ = 8.7 Hz, **H2**), 1.46 (s, 9H, **H24**), 1.30–1.32 (m, 21H, **H22**, **H26**).

^{13}C NMR (75 MHz, THF-D$_8$, 25 °C): δ 170.2 (**C1**), 165.6 (**C20**), 156.0 (**C7**), 155.8 (**C14**), 144.5 (**C13**), 144.0 (**C8**), 143.7 (**C5**), 141.3 (**C19**), 140.3 (**C3**), 137.2 (**C17**), 130.5 (**C18**), 127.8 (**C16**), 127.3 + 127.2 (**C10 + C11**), 122.0 (**C4**), 121.6 (**C6**), 121.4 (**C2**), 120.7 (**C15**), 115.9 + 115.7 (**C9 + C12**), 83.7 (**C25**), 36.3 (**C23**), 34.7 (**C21**), 31.5 (**C24**), 29.8 (**C26**), 25.1 (**C22**).

MS (FAB$^+$, HRMS) *m*/*z* 611.2582 [M]$^+$ (calculated: 611.2591).

Elemental analysis: found: C 66.81, H 6.76, N 4.58, O 10.5 (calculated: C 67.09, H 6.83, N 4.65, O 10.1).

Procedure for the Suzuki-Miyaura-cross-coupling

Stock-solutions of the four precursors were prepared, each in 15 mL of absolute THF: **4**: 306 mg, 0.602 mmol, **5**: 334 mg, 0.592 mmol, **6**: 330 mg, 0.595 mmol and **7**: 366 mg, 0.599 mmol. A stock-solution of the catalyst Pd(PPh$_3$)$_4$ (310 mg, 0.268 mmol in 25 mL of THF) was also prepared. For the four coupling-reactions, 5 mL each of a Br-precursor-solution, a pinacolborane-precursor solution and the catalyst solution were put into a screw-cap flask, treated with 2 mL of a 2 M solution of potassium carbonate in water and stirred at 70 °C for 24 h. Thereafter, the solvent was removed *in vacuo*, the residue suspended in methanol, filtered off, washed with water, methanol and diethyl ether and dried *in vacuo*. The raw product was then dissolved in pyridine, filtered over Celite and crystallized by the addition of *n*-hexane. Yields: **4** + **6**: 95 mg, 0.11 mmol, 56%; **4** + **7**: 121 mg, 0.13 mmol, 66%; **5** + **6**: 119 mg, 0.13 mmol, 66%; **5** + **7**: 177 mg, 0.183 mmol 93%.

Due to very low solubility of all four coupling-products, only ^{1}H-NMR-spectra could be obtained.

8:

^{1}H NMR (300 MHz, DMSO-d$_6$, 25 °C): δ 8.84 (s, 2H), 8.76 (s, 2H), 8.11–8.05 (m, 4H), 7.83 (d, $^4J_{H–H}$ = 2.5 Hz, 2H), 7.64 (dd, $^3J_{H–H}$ = 9.0 Hz, $^4J_{H–H}$ = 2.6 Hz, 2H), 7.55 (d, $^4J_{H–H}$ = 2.6 Hz, 2H), 7.43 (dd, $^3J_{H–H}$ = 8.9 Hz, $^4J_{H–H}$ = 2.7 Hz), 7.34–7.31 (m, 4H), 7.00 (d, $^3J_{H–H}$ = 8.9 Hz), 6.88 (d, $^3J_{H–H}$ = 9.0 Hz), 1.34 (s, 18H).

MS (MALDI$^+$, DHB) *m*/*z* 911.3 [M + H]$^+$ (calculated: 911.3), 933.3 [M + Na]$^+$ (calculated: 933.2), 949.3 [M + K]$^+$ (calculated: 949.2). For simulated isotope pattern match, see Fig. S15.†

Elemental analysis: found: C 67.0, H 5.04, N 6.44, O 7.66 (calculated: C 67.3, H 4.94, N 6.54, O 7.47).

9,10:

^{1}H NMR (300 MHz, THF-d$_8$, 25 °C): δ 8.68 (s, 1H), 8.61 (s, 1H), 8.49 (s, 1H), 8.47 (s, 1H), 8.03–7.97 (m, 2H), 7.93–7.89 (m, 2H), 7.61–7.50 (m, 4H), 7.40 (d, $^4J_{H–H}$ = 2.5 Hz), 7.38–7.33 (m, 2H), 7.23–7.16 (m, 6H), 6.98 (d, $^3J_{H–H}$ = 8.9 Hz), 6.91 (d, $^3J_{H–H}$ = 8.9 Hz), 6.86 (d, $^3J_{H–H}$ = 8.8 Hz), 1.49 (s, 9H), 1.32 (s, 9H), 1.31 (s, 9H).

MS (MALDI$^+$, DHB) *m*/*z* 911.3 [M + H]$^+$ (calculated: 911.3), 933.3 [M + Na]$^+$ (calculated: 933.2), 949.3 [M + K]$^+$ (calculated: 949.2). For simulated isotope pattern match, see Fig. S15.†

Elemental analysis: found: C 67.4, H 5.59, N 6.11 (calculated: C 68.5, H 5.52, N 6.14).

11:

^{1}H NMR (300 MHz, THF-d$_8$, 25 °C): δ 8.71 (s, 2H), 8.55 (s, 2H), 8.03–7.95 (m, 4H), 7.67 (s, 2H), 7.63–7.59 (m, 2H), 7.40 (s, 2H), 7.25–7.22 (m, 6H), 6.99–6.96 (m, 2H), 1.48 (s, 18H), 1.32 (s, 18H).

MS (MALDI$^+$, DHB) *m*/*z* 966.4 [M]$^+$ (calculated: 966.3), 989.3 [M + Na]$^+$ (calculated: 989.3). For simulated isotope pattern match, see Fig. S15.†

Elemental analysis: found: C 69.2, H 6.00, N 5.66, O 6.72 (calculated: C 69.5, H 6.04, N 5.79, O 6.61).

Computational details

DFT-calculations were performed using the Gaussian09 software-package[46] with the B3-LYP hybrid-functional and def2-TZVP basis for all atoms.[47] The geometries were optimized using crystal structural data as the starting values, where available. To evaluate whether the optimized geometries are indeed the global energy-minimum, frequency analyses were carried out and checked for negative force constants. In the calculation for the putative coplanar structure **8C$_i$**, one imaginary frequency at i42 cm^{-1} is observed and characterizes this state as a transition state. The corresponding normal mode represents torsion of the biphenylic bond.

Based on the optimized structures, TD-DFT-calculations were performed. Calculation of the first 25 and 30 states for the mono- and dinuclear compounds proved to sufficiently reproduce the experimental spectra. A shift in the spectra of compounds **6** and **7** of *ca.* 25 nm between the experimental and calculated transitions is observed. This is attributed to solvation effects, which were not taken into account in the calculations.

Acknowledgements

The DFG (SFB 668-TPA4) is gratefully acknowledged for financial support. The Regionales Rechenzentrum as well as the Computing Cluster of the Inorganic Chemistry Institute are acknowledged for generous support and computing time. We thank Dr Daniel Sieh for help with cyclic voltammetry measurements. We also thank Prof. Dr Peter Burger for generous support and discussions. MHP wishes to thank the DFG funded Collaborative Research Center 3MET.de (TRR-88) for funding.

Notes and references

1 R. M. Clarke and T. Storr, *Dalton Trans.*, 2014, **43**, 9380–9391.

2 J. Y. Yang and D. G. Nocera, *J. Am. Chem. Soc.*, 2007, **129**, 8192–8198.
3 A. W. Kleij, M. Kuil, D. M. Tooke, M. Lutz, A. L. Spek and J. N. H. Reek, *Chem. – Eur. J.*, 2005, **11**, 4743–4750.
4 A. K. Crane and M. J. MacLachlan, *Eur. J. Inorg. Chem.*, 2011, **2012**, 17–30.
5 R. G. Konsler, J. Karl and E. N. Jacobsen, *J. Am. Chem. Soc.*, 1998, **120**, 10780–10781.
6 H. Shimakoshi, W. Ninomiya and Y. Hisaeda, *Dalton Trans.*, 2001, **13**, 1971–1974.
7 O. Rotthaus, O. Jarjayes, C. Philouze, C. P. Del Valle and F. Thomas, *Dalton Trans.*, 2009, 1792–1800.
8 M. S. El-Shahawi and W. E. Smith, *Analyst*, 1994, **119**, 327–331.
9 K. Asami, K. Tsukidate, S. Iwatsuki, F. Tani, S. Karasawa, L. Chiang, T. Storr, F. Thomas and Y. Shimazaki, *Inorg. Chem.*, 2012, **51**, 12450–12461.
10 T. Glaser, *Chem. Commun.*, 2011, **47**, 116–130.
11 C. T. Brewer, G. Brewer, G. B. Jameson, P. Kamaras, L. May and M. Rapta, *J. Chem. Soc. Dalton Trans.*, 1995, 37–43.
12 A. Panja, N. Shaikh, P. Vojtíšek, S. Gao and P. Banerjee, *New J. Chem.*, 2002, **26**, 1025–1028.
13 H. Shimakoshi, S. Hirose, M. Ohba, T. Shiga, H. Okawa and Y. Hisaeda, *Bull. Chem. Soc. Jpn.*, 2005, **78**, 1040–1046.
14 A. DiLullo, S.-H. Chang, N. Baadji, K. Clark, J.-P. Klöckner, M.-H. Prosenc, S. Sanvito, R. Wiesendanger, G. Hoffmann and S.-W. Hla, *Nano Lett.*, 2012, **12**, 3174–3179.
15 J. Oldengott, A. Stammler, H. Bögge and T. Glaser, *Dalton Trans.*, 2015, **44**, 9732–9735.
16 M. Bazarnik, B. Bugenhagen, M. Elsebach, E. Sierda, A. Frank, M. H. Prosenc and R. Wiesendanger, *Nano Lett.*, 2016, **16**, 577–582.
17 S. J. Wezenberg, G. Salassa, E. C. Escudero-Adán, J. Benet-Buchholz and A. W. Kleij, *Angew. Chem., Int. Ed.*, 2010, **50**, 713–716.
18 A. C. W. Leung and M. J. MacLachlan, *J. Mater. Chem.*, 2007, **17**, 1923–1932.
19 O. Rotthaus, O. Jarjayes, F. Thomas, C. Philouze, E. Saint-Aman and J.-L. Pierre, *Dalton Trans.*, 2007, 889–895.
20 H. Houjou, M. Ito and K. Araki, *Inorg. Chem.*, 2009, **48**, 10703–10707.
21 T. J. Dunn, C. F. Ramogida, C. Simmonds, A. Paterson, E. W. Y. Wong, L. Chiang, Y. Shimazaki and T. Storr, *Inorg. Chem.*, 2011, **50**, 6746–6755.
22 A. J. Gallant, J. H. Chong and M. J. MacLachlan, *Inorg. Chem.*, 2006, **45**, 5248–5250.
23 R. M. Haak, A. M. Castilla, M. Martinez Belmonte, E. C. Escudero-Adan, J. Benet-Buchholz and A. W. Kleij, *Dalton Trans.*, 2011, **40**, 3352–3364.
24 A. Suzuki, *J. Organomet. Chem.*, 1999, **576**, 147–168.
25 N. Miyaura, K. Yamada and A. Suzuki, *Tetrahedron Lett.*, 1979, **20**, 3437–3440.
26 N. Latif, N. Mishriky and F. M. Assad, *Recl. Trav. Chim. Pays-Bas*, 1983, **102**, 23–77.
27 S. Madhupriya and K. P. Elango, *Synth. React. Inorg., Met. –Org., Nano–Met. Chem.*, 2014, **44**, 1104–1114.
28 J. Lu, Z.-Z. Guan, J.-W. Gao and Z.-H. Zhang, *Appl. Organomet. Chem.*, 2011, **25**, 537–541.
29 F. H. Allen, *Acta Crystallogr., Sect. B: Struct. Sci.*, 2002, **58**, 380–388.
30 A. Hargreaves and S. H. Rizvi, *Acta Crystallogr.*, 1962, **15**, 365–373.
31 J. Poater, M. Solá and F. M. Bickelhaupt, *Chem. – Eur. J.*, 2006, **12**, 2889–2895.
32 D. H. Brown, J. H. Morris, G. Oates and W. E. Smith, *Spectrochim. Acta, Part A*, 1982, **38**, 333–338.
33 J. W. E. Acree and J. S. Chickos, *NIST Chemistry WebBook, NIST Standard Reference Database Number 69*, National Institute of Standards and Technology, Gaithersburg, MD, 2011, p. 20899.
34 P. S. G. E. Staff, *UV Atlas of Organic Compounds*, Springer Science + Business Media, 1967.
35 F. Almasy and H. Laemmel, *Helv. Chim. Acta*, 1950, **33**, 2092–2100.
36 R. Bauernschmitt and R. Ahlrichs, *Chem. Phys. Lett.*, 1996, **256**, 454–464.
37 S. Kuck, S.-H. Chang, J.-P. Köckner, M. H. Prosenc, G. Hoffmann and R. Wiesendanger, *ChemPhysChem*, 2009, **10**, 2008–2011.
38 B. E. C. Bugenhagen, L. Brinn and M. H. Prosenc, *Organometallics*, 2014, **33**, 7015–7018.
39 A. Choudhary, B. Das and S. Ray, *Dalton Trans.*, 2015, **44**, 3753–3763.
40 R. L. Martin, *J. Chem. Phys.*, 2003, **118**, 4775–4777.
41 Y. Nishida and S. Kida, *Chem. Lett.*, 1973, **2**, 57–62.
42 O. Rotthaus, F. Thomas, O. Jarjayes, C. Philouze, E. Saint-Aman and J.-L. Pierre, *Chem. – Eur. J.*, 2006, **12**, 6953–6962.
43 O. Rotthaus, O. Jarjayes, F. Thomas, C. Philouze, C. Perez Del Valle, E. Saint-Aman and J.-L. Pierre, *Chem. – Eur. J.*, 2006, **12**, 2293–2302.
44 M. L. Olmstead and R. S. Nicholson, *Anal. Chem.*, 1966, **38**, 150–151.
45 R. S. Nicholson, *Anal. Chem.*, 1966, **38**, 1406–1406.
46 M. J. Frisch, *et al.*, *Gaussian 09, Rev. D01*, Gaussian Inc., Wallingford, CT, 2009.
47 F. Weigend and R. Ahlrichs, *Phys. Chem. Chem. Phys.*, 2005, **7**, 3297–3305.

